Tailoring properties of platinum supported catalysts by irreversible adsorbed adatoms toward ethanol oxidation for direct ethanol fuel cells

Marta C. Figueiredo [a], Annukka Santasalo-Aarnio [a], Francisco J. Vidal-Iglesias [b], José Solla-Gullón [b], Juan M. Feliu [b], Kyosti Kontturi [a], Tanja Kallio [a,*]

[a] Fuel Cell Research Group, Department of Chemistry, School of Chemical Technology, Aalto University, FI-00076 AALTO, Finland
[b] Instituto Universitario de Electroquímica, Universidad de Alicante, Apt 99, 03080 Alicante, Spain

ABSTRACT

In this work ethanol oxidation on carbon supported Pt catalysts modified with irreversibly adsorbed adatoms is reported. This study concerns understanding of the effect of a second metal on real catalysts in conditions as close as possible to those applied in fuel cells systems. The results were acquired using cyclic voltammetry, chronoamperometry and *in situ* infra-red techniques always taking into account the future application of the electrocatalyst materials in fuel cells. Foreign adatoms, both Bi and Sb, irreversibly adsorbed on a Pt electrode were studied, and revealed to enhance catalytic activity toward a more efficient ethanol oxidation. The catalytic enhancement continuously increased with the coverage of the adatom on the surface up to coverages close to saturation. With these high coverages a decrease of the activity was observed suggesting that free platinum atoms are required to oxidize ethanol. The results suggest that the adatoms play a third body role avoiding the poisoning of the Pt sites that will then be free for oxidizing ethanol. However, electronic effects on Pt/C–Bi and bifunctional mechanism at Pt/C–Sb are also suggested. The oxidation products were identified by *in situ* FTIR and are mainly acetaldehyde and acetic acid for the three catalysts. CO_2 was also observed for the unmodified Pt/C and interestingly for the Pt/C–Sb electrodes.

© 2013 Elsevier B.V. All rights reserved.

1. Introduction

The direct alcohol fuel cell (DAFC) has emerged in the last decades as a promising alternative power source for portable applications. The biggest advantages of the use of alcohols as fuels instead of hydrogen are their easy storage (liquid state) and high theoretical mass energy density [1,2]. The most studied alcohol for these applications has been methanol. However, ethanol offers an attractive alternative due to its lower toxicity and a possibility to be produced in large quantities from biomass. Nevertheless, the direct ethanol fuel cells (DEFCs) have also encountered some difficulties associated with their low efficiency due to the incomplete oxidation to CO_2.

Electro-oxidation of ethanol can occur by different reaction pathways (Scheme 1). If the reaction is complete and CO_2 is the final product twelve electrons per molecule are produced, which is two times that produced by complete oxidation of methanol, for example. However, some 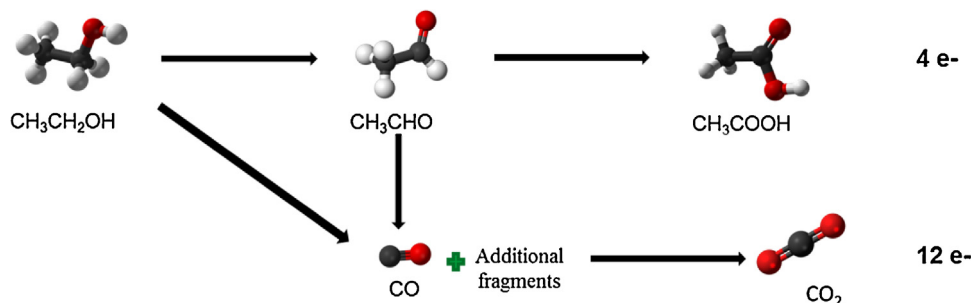pathways lead to the formation of partially oxidized products (as acetaldehyde and acetic acid) due to the difficulty of breaking the C—C bond. These intermediates subsequently desorb from the surface and do not undergo further oxidation resulting in loss of efficiency.

Acetaldehyde and acetic acid have been found as the major products of ethanol oxidation in a wide range of catalysts [3] which limits the potential performance of the fuel cell. In addition, the formation of acetic acid is not desired in a fuel cell because it also causes local changes in the pH of the anode decreasing the membrane life time. By these reasons further investigation to understand the reaction mechanism and to find more efficient catalysts that can promote the total oxidation of ethanol to CO_2 are required.

One efficient way to induce new catalytic properties is the use of bimetallic surfaces. Materials, such as PtSn [4], PtRh [5], and PtRu [1,6,7], have been widely used for ethanol oxidation and in many cases the improvement of the reactivity is noticeable. One simple way to produce bimetallic surfaces is by irreversible adsorption of adatoms on the Pt surface. Many elements of the sp group can be spontaneously adsorbed on the Pt surface just by putting it in contact with a solution containing the respective salt. These surfaces are normally stable in a large potential range. A successful example

* Corresponding author. Tel.: +358 505637567; fax: +358 947022580.
E-mail address: Tanja.kallio@aalto.fi (T. Kallio).

Scheme 1. Proposed mechanisms for ethanol oxidation on Pt.

of the enhancement of the catalytic properties of platinum surfaces by the deposition of irreversible adsorbed adatoms was found on the oxidation of formic acid [8,9], methanol [10] and also ethanol [11–13] at Pt single crystals. These reactions also proceed through a dual-path mechanism. Adatom modification can affect each of these pathways independently, the effect normally sought being inhibition of the poisoning reaction and enhancement of the direct oxidation reaction.

In this work we report the use of carbon supported platinum nanoparticles modified by irreversible adsorption of Bi and Sb for ethanol oxidation. The experiments were performed and results obtained in very similar conditions to those that would be applied in fuel cell tests, aiming to obtain useful information about activity and durability of the catalyst for further *in situ* applications. Moreover, the reaction products and intermediates were examined by *in situ* infrared spectroscopy. The main products found on the modified electrodes were acetaldehyde and acetic acid. Although these are not the desirable products for fuel cell applications, here is demonstrated that platinum catalysts properties can be tailored by simple and easy to do methods, favoring the reaction toward one of the many possible paths. However, the lower poisoning rate was demonstrated for these catalysts in both the cases. This is definitely an advantage for fuel cells application. Nevertheless, the understanding of the reactions is one of the most important steps for the design of new catalysts.

2. Experimental

The synthesis of the nanoparticles supported on carbon (20 wt%) was done as described in a previous report [14]. Very briefly, sodium citrate, H_2PtCl_4 and sodium borohydride were used as stabilizer, metallic precursor and reducing agent, respectively. After the reduction step, the carbon Vulcan XC-72R was added under fast stirring, alternating both magnetic and ultrasonic for about 2 h, in order to properly disperse the hydrophobic carbon in the water solution, and also to favor the homogeneous adsorption of the nanoparticles on the solid surface. Once the nanoparticles were adsorbed on the carbon surface, some NaOH pellets were added to the mixture, in order to precipitate the solid, and the synthesis mixture was left to stay overnight. After complete precipitation, the sample was filtered and rinsed, at least 4–5 times, with ultra-pure water to make sure that a clean sample, without any reactant adsorbed on the surface, was obtained.

The mean size of the particles was about 2.2 ± 0.5 nm measured by transmission electron microscopy (TEM). These experiments were performed with a JEOL JEM-2010 microscope working at 200 kV (Fig. 1). The sample for TEM analysis was obtained by placing a drop of the dispersed solution onto a Formvar-covered copper grid and evaporating it in air at room temperature.

An ink for the electrochemical experiments was prepared using 5 mg of carbon supported Pt catalyst, 20 μl of Nafion® solution (5 wt% Aldrich) and 200 μl of ethanol (p.a., Altia) that were carefully mixed with a magnetic stirrer and an ultrasonic bath. The experiments were performed in a classical three electrode cell at controlled temperature of 20 °C and under nitrogen purge (5.0 from AGA gases). A platinum coil was used as counter electrode and a reversible hydrogen electrode as a reference. The working electrode was prepared by deposition of 4 μl of the ink onto a glassy carbon electrode (0.1963 cm^2 of geometric area) previously cleaned by polishing with an alumina solution and putting in the ultrasonic bath. The electrodes prepared with this procedure will have a Pt loading of ∼0.02 mg. The experiments were performed with a potentiostat/galvanostat PGSTAT100 Autolab system and a rotating device from Pine Instruments.

The electrochemical characterization and cleaning of the carbon supported Pt nanoparticles was performed in a 0.1 M H_2SO_4 solution at room temperature. Following the procedure previously described [15], prior to the use of the nanoparticles for ethanol oxidation, they were cleaned by CO adsorption and stripping, after which the base voltammograms were recorded in 0.1 M H_2SO_4 not only to calculate the real surface area of the catalyst but also to assess the surface cleanliness by simple examination of the voltammograms [16]. The active surface area of the Pt nanoparticles was determined by the charge involved in the so-called hydrogen UPD region assuming 0.23 mC cm^{-2} for the total charge after the subtraction of the conventional current attributed to double layer charging contribution [16].

The adatom layer was adsorbed on the electrode surfaces by putting it in contact with a 0.1 M H_2SO_4 solution containing 10^{-5} M of the correspondent salt (Bi_2O_3 or Sb_2O_3) at open circuit. The electrode was then rinsed with ultra-pure water and transferred to the cell containing the supporting electrolyte (0.1 M H_2SO_4) where the voltammogram was recorded.

The surface coverage of the adatoms was measured according with previously reported methods ([17] for Bi and [18] for Sb). Different coverages were obtained by different immersion times and different adatom concentrations on the acidic solution. Then the electrode was transferred to the electrochemical cell containing 1 M of ethanol in 0.1 M $HClO_4$ where the catalysis was evaluated. The stability of the modified electrode was achieved by comparing the blank CV after ethanol oxidation with the one obtained before (no significant differences were found for both Bi and Sb).

As usual [7,17] Fourier-transform infrared spectroscopy (FTIRS) experiments were performed with a Nicolet Magna 850 spectrometer, equipped with an MCT detector. The spectroelectrochemical cell was provided with a prismatic CaF$_2$ window beveled at 60°. Spectra shown are composed of 100 interferograms collected with a resolution of 8 cm^{-1} and p-polarized light. They are presented as absorbance, according to $A = \log(R/R_0)$, where R and R_0 are the reflectance corresponding to the single beam spectra obtained at the sample and reference potentials, respectively. All the spectroelectrochemical experiments were conducted at room temperature, with a reversible hydrogen electrode (RHE) and a platinum wire used as the reference and counter
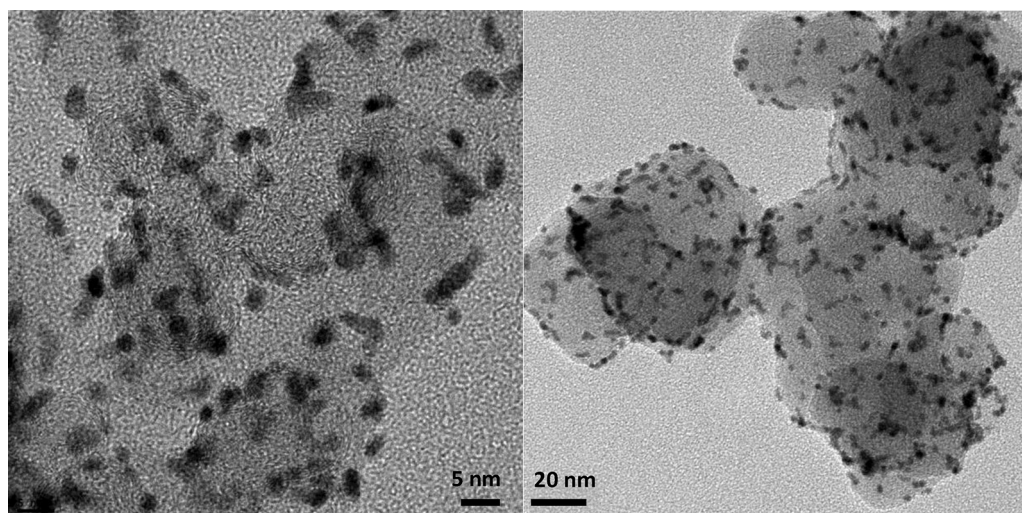
Fig. 1. TEM micrographics from the Pt/C used in this study.

electrodes, respectively. For these experiments a gold collector electrode was used and the catalyst inks were prepared without the ionomer (Nafion) in order to avoid the undesirable bands coming from the polymer.

3. Results and discussion

3.1. Pt/C modified with Bi

The use of modified surfaces has been described as a good approach for the increase of the catalytic properties of platinum surfaces for several electrocatalytic applications [8,10,17]. Studies concerning fuel cell anode reactions have also been reported in modified single crystal surfaces [8,10], preferentially oriented nanoparticles and also carbon supported nanoparticles [9,17,19,20].

In Fig. 2 the blank CV for the nanoparticles (after cleaning) and for the different Bi coverages used are given. The CV for the clean particles shows clearly the H adsorption region for potentials below 0.4 V characteristic from Pt surfaces. In this region, two peaks can be distinguished at 0.20 and 0.32 V (in the positive scan). These features are typical from polyoriented Pt nanoparticles although they are expected to be sharper and more reversible according to previous publications of particle synthetized by the same method [14].

It was observed that the presence of the ionomer in the ink deposited on the electrode decreases the sharpness and the

reversibility of H adsorption peaks because of hindered mass transfer from the solution to the catalyst surface. However, the main aim of our work is to mimic in the electrochemical cell the conditions that are used in fuel cells and therefore the inks have the same chemical content and ratios as those prepared for the *in situ* fuel cell experiments.

When Bi is adsorbed on the electrode surface the H adsorption region decreases together with the progressive appearance of a redox couple at high potentials, 0.67 V, due to the Bi redox process. The results agree with previous reports of Bi adsorption on carbon supported nanoparticles [9].

Fig. 3 shows the results obtained for ethanol oxidation on the Pt/C nanoparticles modified with different Bi coverages. The results were obtained in unstirred solutions as well as under electrode rotation in order to be closer to the real conditions in a fuel cell anode, were the solution is always flowing through the catalyst layer avoiding mass transport limitations for the electrode reactions.

The results show that the presence of Bi on the surface leads to the increase of the current densities for ethanol oxidation. The high coverage (0.91) of the adatom increases the current almost 3 times when compared with the unmodified electrode. However, for coverages close to the full monolayer of Bi on the surface the catalytic activity abruptly decreases indicating that Bi–Pt pairs are needed for the electrocatalytic oxidation reaction and that Bi is not active by itself.

In general the enhancement can be explained by tree main factors [21–23]: change in the electronic properties of the substrate, ensemble or third body effects arising from the selective blockage of a particular adsorption site or bifunctional catalysis. In addition, it is well known from the literature [24], that there are many residues formed when ethanol is adsorbed on platinum. Iwasita reported [24] that species other than CO, containing C, O, H can be strongly adsorbed on the electrode surface acting as catalyst poisons.

It has been proposed that at least two contiguous free Pt sites are required for CO formation [25]. The enhancement of the catalytic activity with the Bi coverage can be explained by considering that the adatoms break the existence of a particular ensemble of sites on the surface in which poison formation can take place [8]. The remaining free Pt sites on the surface, which are not available for poison formation, would be still active for the direct oxidation of ethanol. For low coverages, the activity remains low, since the probability of having enough number of adjacent Pt atoms to allow poison formation would still be high. It can be assumed that Bi is avoiding the poisoning of the surface (from CO or other C, O and H
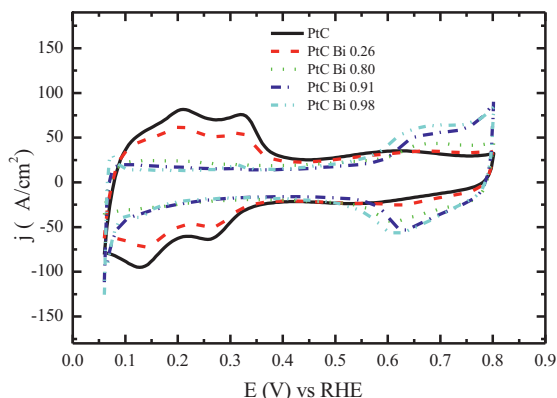

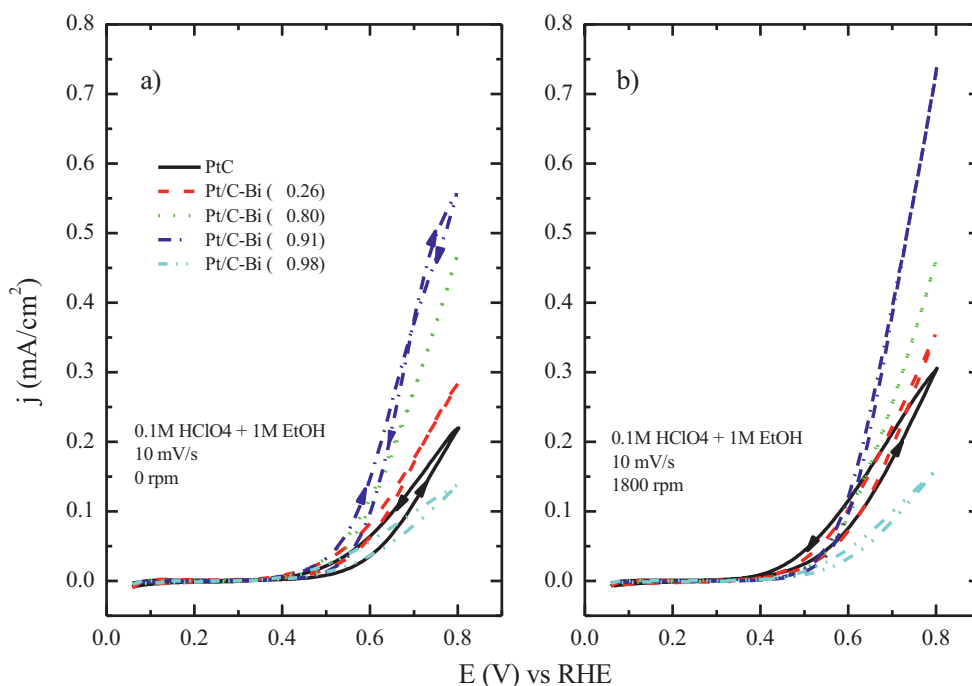**Fig. 2.** CVs for Pt/C with different Bi coverages in 0.1 M H_2SO_4 at 50 mV/s.

Fig. 3. Cyclic voltammograms for Pt/C with different Bi coverages (0, 0.26, 0.80, 0.91 and 0.98) in 1 M of ethanol in 0.1 M HClO$_4$, (a) 0 rpm and (b) 1800 rpm.

containing species) through this third body effect, allowing ethanol to be oxidized at the same potential range on platinum. Moreover, the fact that the activity increases till very high coverages of Bi are reached supports a third body effect of Bi for the reaction as it was previously demonstrated for formic acid oxidation at well-defined platinum surfaces modified with this adatom at Pt(1 0 0) and Pt(1 1 0) electrodes [8].

In addition, the shape of the CV is not affected by the presence of the adatom although the hysteresis of the reactions seems to decrease with increasing coverages. It has been shown that the hysteresis is associated with the formation of strongly adsorbed species, mainly CO, which are formed on the electrode surface at low potentials [7]. These adsorbed species remain at the electrode surface till high enough potentials are reached and they can be oxidized (above 0.6–0.7 V). Then, the electrode surface becomes free what causes an increase in the oxidation currents on the negative going scan [26]. The fact that the hysteresis phenomenon decreases (up to the same upper potential limit and sweep rate) in the presence of the adatom indicates a lower degree of poisoning of the electrode surface.

It is also important to remark that, when there is no transport limitation (rotating the working electrode, Fig. 3b) an undesirable shift toward more positive potentials for the potential onset of the reaction is observed and the increase of the activity is not as high as in the steady state case. This suggests that in addition to the third body effect, also some other (negative) effects like changes on electronic properties may exist.

It has been demonstrated that the presence of Bi on Pt single crystals changes the electronic properties of the surface increasing the electronic back donation (Bi donates electrons to Pt, causing an increase in the extent of d$\pi_{Pt} \rightarrow 2\pi^*_{CO}$ [27]) stabilizing the adsorbed CO molecule and no catalytic effect is expected from this system toward CO oxidation [28,29]. The stabilization of CO on Pt surfaces by the presence of Bi can be observed experimentally with Fourier transform infrared (FTIR) measurements [30] by the displacement of the CO stretching band to lower wavenumbers and by the change in the dependence of the band frequency on electrode potential, with the slope dυ/dE increasing for the adatom-modified surfaces. Taking these considerations into account, it is suggested that the

shift on the potential onset of this reaction is due to stabilization of the species at the surface by change on the electronic properties of the system. This suggests that although the poison formation on the surface occurs in lower extent, the remaining is oxidized latter and therefore no improvement on the onset potential is observed. Unfortunately, on the ethanol oxidation reaction separation of the direct 12 electron transfer path from the poisoning reaction is difficult, since this reaction can only be studied in solutions containing ethanol, and hence both reaction pathways will take place simultaneously. Therefore, it is difficult to draw further conclusions under these experimental observations.

On the other hand, if we think in a bifunctional catalytic effect the shift on the potential onset can be explained by the fact that the oxidation of Bi starts around 0.6 V and at this potential the adatom can donate oxygenated species for a more efficient oxidation of ethanol. In this case, ethanol and CO oxidation will take place coupled with the adatom.

Chronoamperometric measurements at a fixed potential were performed in order to get further insight into catalyst poisoning [31]. The electrode potential was stepped from 0.1 to 0.6 V and was held at this potential (at which ethanol oxidation currents are observed in the CV) for over 30 min (2000 s) and the current was recorded. As it is observed in Fig. 4, the current after 2000 s increases with the Bi concentration on the surface of the Pt/C electrode until coverage values of 0.98 are reached. For this high coverage, the number of free Pt sites available for ethanol oxidation is to low leading to the decrease of the current intensity in all the time range. For the other coverages the increase in current is high for the first 500 s but after that the poisoning of the surface appears, and, although the currents are higher after 2000 s, they are very close to the ones obtained for the clean Pt. These results are very important for fuel cell applications where the catalyst activity for long periods of time is essential.

3.2. Pt/C modified with Sb

Sb has been reported as an oxygen donor adatom [32], which has a bifunctional catalytic effect on CO oxidation shifting the onset potential of the oxidation to lower values because the adatom redox
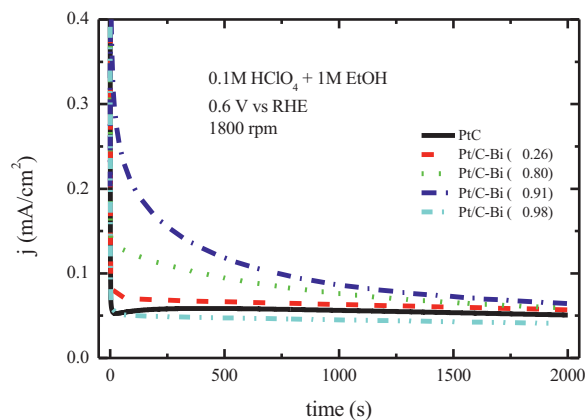
Fig. 4. Chronoamperometric curves for Pt/C and Pt/C with different Bi coverages for 2000 s at 0.6 V (*vs.* RHE).

Fig. 5. CVs for Pt/C with different Sb coverages in 0.1 M H$_2$SO$_4$ at 50 mV/s.

process occurs at lower potentials [33]. By this reason the study and comparison of Sb with Bi as adatoms at platinum surfaces for ethanol oxidation will help to shed light into the increase of the activity of the reaction at the modified surfaces.

Fig. 5 shows the voltammetric curves in 0.1 M sulphuric acid for Pt/C modified with different coverages of irreversibly adsorbed Sb. In agreement with previous reports [18,34] the results show that the increase of the Sb coverage on the surface causes a decrease in the hydrogen adsorption region together with the appearance of a broad redox process between 0.45 and 0.55 V (*vs.* RHE). The upper potential limit was kept at 0.6 V in order to avoid Sb dissolution from the surface, which starts to become critical at potentials above 0.8 V [33].

After electrochemical characterization, these modified surfaces were again transferred to another electrochemical cell with ethanol in solution and their catalytic activity was evaluated. Results are given in Fig. 6.

Similarly to Bi, the presence of Sb on the surface of the Pt catalyst increases the oxidation currents for ethanol. The shape of the CV
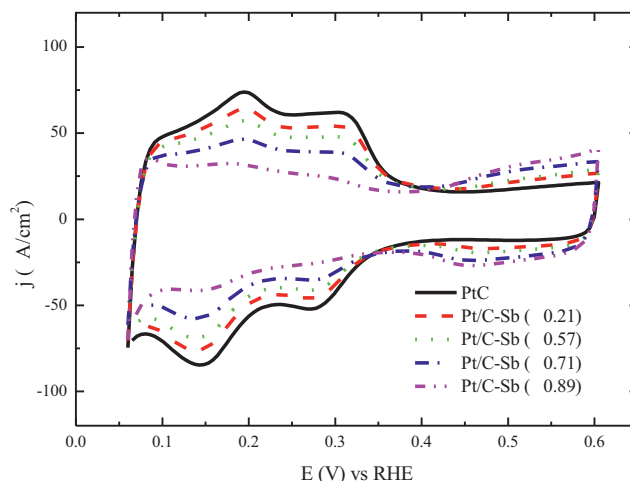
is practically the same in the presence and absence of the adatom although the hysteresis slightly decreases (positive and negative sweeps show almost the same currents). It is important to notice that, in this particular case, the onset potential of the reaction is shifted to lower potentials (even when rotating the electrode) just when the adatom starts oxidizing, suggesting some differences in the activity of the two adatoms. As it has been referred before for Bi, the electronic effect, bifunctional mechanism or external third body effect can explain the increase on the catalytic effect of Sb on Pt toward ethanol oxidation.

Previous reports [35] for single crystals show that for CO oxidation almost no displacement of the vibrational band is observed in the presence of Sb, indicating that electronic effects are very weak in these cases. However, a bifunctional mechanism through an adatom-mediated oxygen transfer can explain the shift on the onset potential to lower values when Sb is present on the electrode surface. The adsorbed Sb has an oxidation potential lower
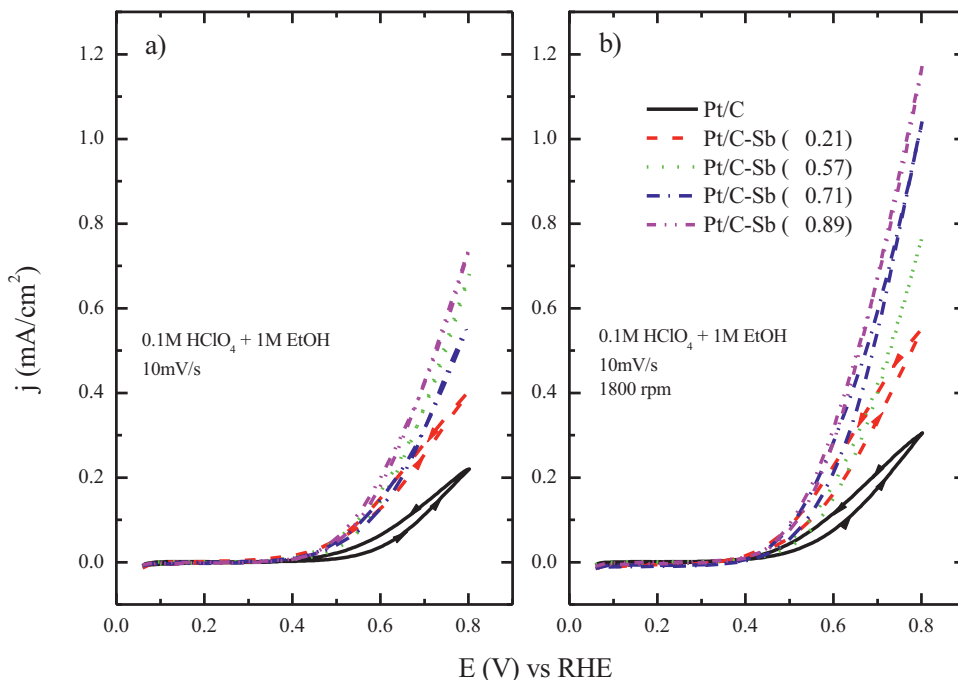

Fig. 6. Cyclic voltammograms for Pt/C and Pt/C–Sb (θ 0.21, 0.57, 0.71 and 0.89) in 1 M of ethanol with 0.1 M HClO$_4$, (a) 0 rpm and (b) 1800 rpm.
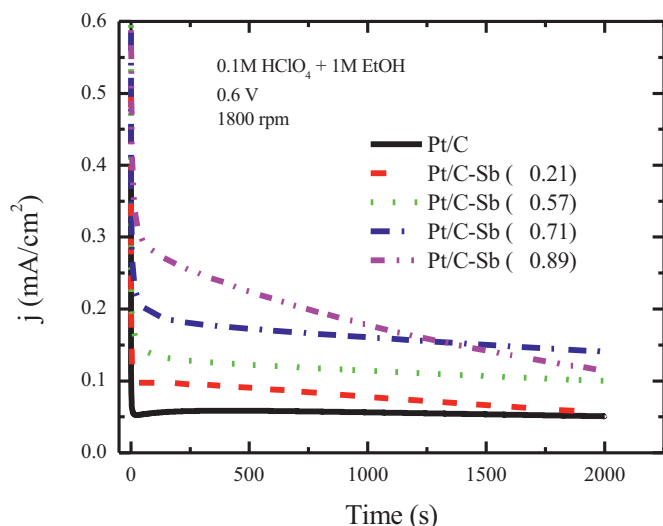
Fig. 7. Chronoamperometric curves for Pt/C, Pt/C–Sb (θ 0.21, 0.57, 0.71, 0.89) for 2000 s at 0.6 V (*vs.* RHE).

than ethanol or CO meaning that oxygen will be available at the surface at lower potential allowing the reaction to proceed easier.

Despite these differences, the similarities on the catalytic behavior of the two adatoms support the previously described assumption of the third body effect. At some extent, the adatom (independently of its chemical nature) is acting as an "external body" that blocks a particular ensemble of sites on the surface preventing the poison formation. In this way, Pt sites free from poison will exist on the surface and thus being able to oxidize ethanol. The FTIR experiment presented latter will help on the understanding of this differences in a mechanistic point of view.

The chronoamperometric results reported in Fig. 7 show that the currents at 0.6 V increase with the increase of Sb at the surface of the Pt/C catalyst. However, for coverages as high as 0.89 the current is still pretty high on the first 500 s of measurement, but it drops drastically after that, reaching current intensities as low as those for coverages of half of the surface. Comparing to the results for the high Bi coverages this fact can be tentatively explained by suggesting that the number of free Pt sites on the surface is no longer

sufficient to proceed with the reaction and they get poisoned very fast.

3.3. FTIR experiments

The results previously shown do not suggest any dramatic change on the reaction mechanism due to the presence of foreign adatoms. However, the best way to confirm this assumption is to use experimental techniques that allow the identification of the involved intermediates and products. For this, *in situ* FTIR experiments were done on pure Pt surfaces and in the presence of Bi and Sb.

In the following spectra, positive bands correspond to the products formed at the sample, during the ethanol oxidation, while negative bands are due to the consumption of species present at the reference potential. The contact of the electrodes with the ethanol solution was made at a controlled potential of 0.10 V where, apparently, no adsorption or reaction process occurs [36]. This potential was maintained until the electrode was pressed against the CaF$_2$ window. After collecting the reference spectrum, the potential was stepped to progressively higher sample potential values, where the corresponding sample spectra were collected. Those potentials are labeled in the respective figures and captions.

In Fig. 8 the spectra obtained for ethanol oxidation on Pt/C, Pt/C–Bi ($\theta = 0.83$) and Pt/C–Sb ($\theta = 0.67$) at different sample potentials in 1 M EtOH and 0.1 M HClO$_4$ are shown. Several bands can be observed. A broad band between 2500 and 3000 cm^{-1} is observed in all the surfaces studied. This band corresponds to the C—H region (2700–3000 cm^{-1}) and is overlapped with other wide band, due to OH from carboxyl group between 2500 and 3000 cm^{-1} that is expected to exist in the most probable final products of ethanol oxidation [37] (acetic acid and acetaldehyde). These bands become more intense with the increase of the potential due to the higher oxidation rate.

Other observed bands are at 2341 cm^{-1} the C—O asymmetric stretching from CO$_2$ [37,38]; at 1713 cm^{-1} the C=O stretching from carbonyl groups either from acetic acid and acetaldehyde [26]; the bands at 1280, 1370–1390 cm^{-1} from C—O stretching and CH$_3$ bending from acetic acid [26]; the band at 1402 cm^{-1} due to adsorbed acetate ions [26] and, finally a band at 1114 cm^{-1} of CH$_3$ wagging from acetaldehyde [11].
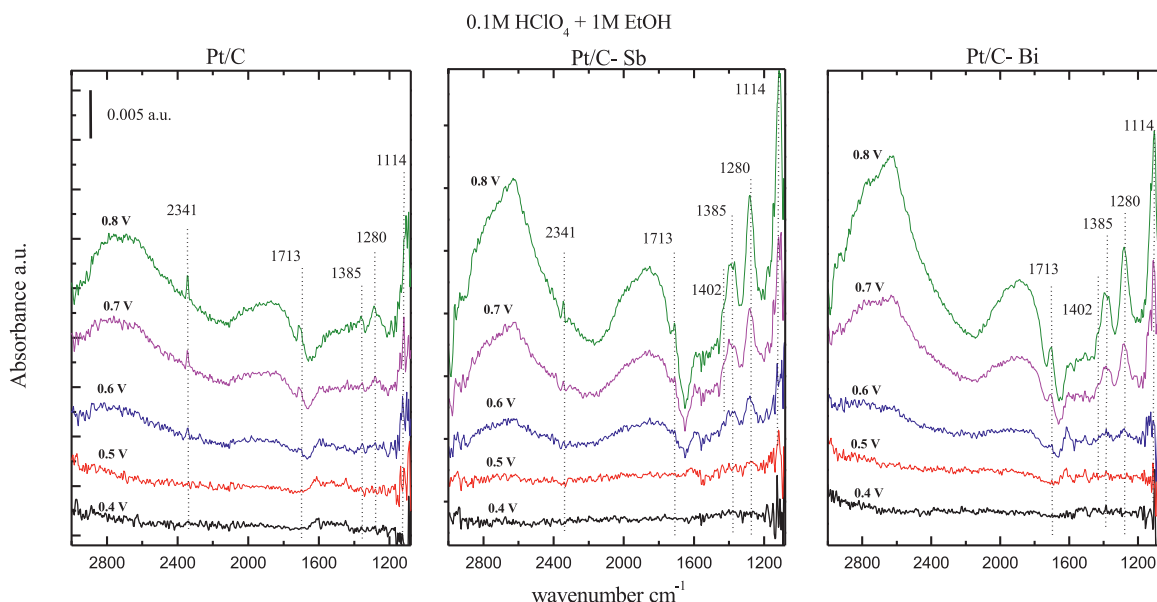
0.1M HClO$_4$ + 1M EtOH

Fig. 8. Spectra obtained for ethanol oxidation (1 M in 0.1 M HClO$_4$) at Pt/C, Pt/C–Sb ($\theta = 0.67$) and Pt/C–Bi ($\theta = 0.83$) obtained with 100 scans at 8 cm^{-1}. E_{ref} 0.1 V.

It is important to notice that CO is not observed on any of the surfaces in the potential range studied. This fact does not mean that CO is absent under these conditions but more likely that the CO oxidation at these potentials is faster than its production and the corresponding IR bands stay below the detection limit. Moreover, it is well known that surface steps/defects enhance the rate of the CO oxidation in platinum surfaces [16,39,40]. On Pt nanoparticles the CO oxidation to CO_2 is expected to be fast due to the small size of the sites and because the surface is formed in majority by defects and steps [16].

Taking a closer look to each of the surfaces separately, we can see that for Pt/C the products of ethanol oxidation start appearing at 0.6 V. First, as expected from comparison with Pt bulk electrodes [26,38] the CO_2 band at 2341 cm^{-1} is observed (at 0.6 V). This band remains up to 0.8 V. When the electrode potential is increased to 0.7–0.8 V the bands related with acetic acid and acetaldehyde can also be observed. Although the band at 1114 cm^{-1} is already very close to the limit of the noise bands from the prismatic window, we can see that the bands at 1280 and 1370–1390 cm^{-1} can only be clearly observed at potentials as high as 0.8 V and the band at 1713 cm^{-1} and 1114 cm^{-1} are already observed at 0.7 V. It can be suggested, based on these results that acetaldehyde is being formed first directly from ethanol and further oxidized to acetic acid, which is the final product.

When the adatoms are present at the surface, the results depend on their chemical nature. In the presence of Sb, the main products of the reaction are the same than those observed for the clean Pt/C electrode, *e.g.* CO_2, acetaldehyde and acetic acid. As aforementioned, no CO band is observed in the spectra. In this case, the bands related with acetaldehyde and acetic acid are more intense that in pure Pt, and the CO_2 band is just observed at very high potentials (0.8 V). These observations suggest that for Pt/C–Sb surfaces, the path that leads to CO_2 from adsorbed CO is inhibited in some degree by the adatom. The obtained CO_2 comes probably from the oxidation of other intermediates different from CO. It is known that the presence of steps catalyzes the C—C bond cleavage at low potentials [29]. Moreover, in the modified surfaces these steps are more blocked by the adatom, shifting the reaction toward ethanol oxidation to acetaldehyde [40].

In the case of Pt/C–Bi, the direct path of ethanol oxidation to CO_2 is totally inhibited once that no band at 2341 cm^{-1} is observed at any potential. Similarly to what occurs with Sb, the formation of acetaldehyde and acetic acid is enhanced at high potentials as showed by the presence of bands at 1713, 1280 and 1370–1390 cm^{-1}.

On both modified electrodes, Pt/C–Bi and Pt/C–Sb, a small shoulder at 1402 cm^{-1} is observed at (0.7–0.8 V) revealing the presence of adsorbed acetate. This can be expected at platinum in presence of acetic acid in the thin layer solution.

A summary of the most important bands from the spectra is presented in Fig. 9. The area of the bands obtained from integration is plotted for acetic acid (only the band at 1280 cm^{-1} is presented because the other one follows the same trend), acetaldehyde (band at 1114 cm^{-1}) and CO_2. This comparison is meaningful as the same Pt/C nanoparticle electrode was used for the three measurements in the following order Pt/C, then Pt/C–Sb and finally Pt/C–Bi. After each measurement the CV of the electrode was taken to ensure that the electrode active area remained unaltered. Thus, after the Pt/C–Sb IR measurements had been done, Sb from the surface was removed by voltammetric stripping. Then, the CV was again checked and finally modified with Bi.

The results show that, as expected from the voltammetric and chronoamperometric data, the Pt/C–Sb surface is the most active for ethanol oxidation at high potentials and the reaction products start appearing at lower potentials than for the other studied surfaces. At 0.6 V, both bands of acetaldehyde and acetic acid start
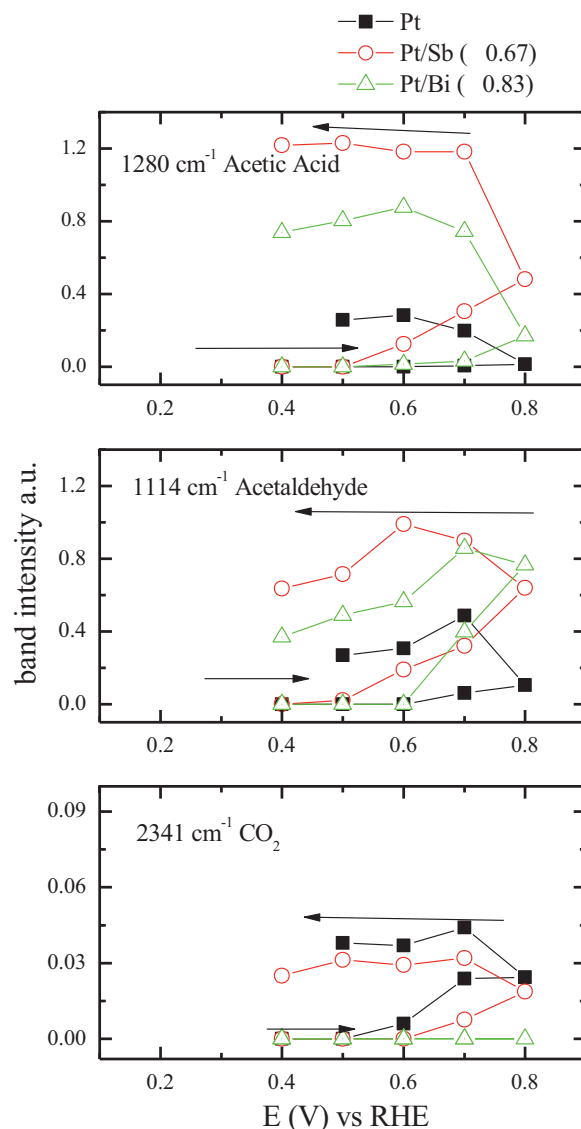

Fig. 9. Integration of the bands at 1280 (acetic acid), 1114 (acetaldehyde) and 2341 cm^{-1} (carbon dioxide) for Pt/C, Pt/C–Bi (θ = 0.83) and Pt/C–Sb (θ = 0.67).

to increase, although it is possible to see that the band related with acetaldehyde is more intense meaning that probably acetaldehyde is formed at the surface at one first stage and then further oxidized to acetic acid. In the negative going sweep, the tendency is changed and acetic acid is the main product. CO_2 band is observed for potentials as high as 0.7 V, although always less intense than in pure platinum.

For the Pt/C–Bi surface, the reaction products are only visible at potentials above 0.7 V. It is interesting to notice that in this case, acetaldehyde bands are more intense than those for acetic acid in almost all the potential range (exception for the potentials below 0.6 V in the negative scan probably due to the accumulation of this species on the thin layer). This fact, together with the absence of CO_2 supports the idea of a third body effect for this adatom. Specific reaction sites will be blocked both for poison formation and further oxidation of acetaldehyde to CO_2 or acetic acid. By contrast, in the case of Pt/C–Sb surfaces, the fact that the reaction starts at lower potentials and that the products are very similar to those obtained for clean Pt supports the idea of a bifunctional mechanism. However, we should have in mind that other effects cannot be totally excluded.

When these results are compared with those obtained for adatoms adsorbed on single crystal electrodes [7,11,12] the effects of the adatoms are slightly different. For example, when Pt single crystals are decorated with Ru adatoms [7,11], low ruthenium coverages on step sites promote the oxidation of CO formed on the steps from the cleavage of the C—C bond. However, high ruthenium coverages have an important inhibiting effect for the cleavage of the C—C bond and the major product in the oxidation process is acetic acid, similarly to the effect of Pt–Sn ensembles [12]. In our studies, none of the adatoms seems to enhance the C—C bond cleavage to CO_2 but they both increase the ethanol oxidation toward acetic acid in the case of Sb and toward acetaldehyde for Bi.

These results are, in any case, very important for the understanding of the ethanol oxidation mechanism in real catalysts used in fuel cells, and they can help in the development of more appropriate ones. Moreover, it was clearly demonstrated that the properties of platinum based catalysts should be tailored for achieving better results, and irreversibly adsorbed adatoms were shown as a fast, easy and simply way to do it.

4. Conclusions

In this work we report the effect of modifying Pt supported catalysts with irreversibly adsorbed adatoms toward ethanol oxidation reaction. The presence both of Bi and Sb showed to increase the catalytic activity of the electrode for this reaction for a wide range of coverages. It was observed that for coverages near saturation the enhancement was decreased by the subsequent poisoning of the remaining Pt atoms or adatom losses. It was demonstrated that the adatoms can have two effects on the surface. Both of them have a role of third body avoiding the formation of adsorbed species that act as poison for the reaction. Together with this effect, changes in the electronic properties of Pt in the case of Bi and a bifunctional mechanism for Sb were also found. In any case, other effects cannot be excluded.

The FTIR experiments showed as reaction products acetaldehyde and acetic acid for all the surfaces (Pt/C, Pt/C–Bi and Pt/C–Sb) and CO_2 for Pt/C and Pt/C–Sb. However, the product distribution revealed to be different in each case. While Pt/C–Sb had acetic acid as main product, acetaldehyde was observed for Pt/C–Bi. This difference on the product distribution with the chemical nature of the adatom supports the idea of different behavior for the catalytic enhancement of the two adatoms. In any case, the presence of a foreigner adatom increased the rate of ethanol oxidation, revealing that this can be an easy and versatile approach for fuel cell application.

The reported results are important for shedding some light on the understanding of the ethanol oxidation mechanism in real catalysts, and can help on the design of more effective ones. Definitely, it was shown that the use of irreversibly adsorbed adatoms is a good approach for tailoring the properties of Pt/C catalyst for ethanol oxidation.

Acknowledgments

References

[1] F. Vigier, S. Rousseau, C. Coutanceau, J. Leger, C. Lamy, Topic in Catalysis 40 (2006) 111–121.
[2] E. Antolini, Journal of Power Sources 170 (2007) 1–12.
[3] A. Santasalo-Aarnio, Y. Kwon, E. Ahlberg, K. Kontturi, T. Kallio, M.T.M. Koper, Electrochemistry Communications 13 (2011) 466–469.
[4] F. Vigier, C. Coutanceau, F. Hahn, E.M. Belgsir, C. Lamy, Journal of Electroanalytical Chemistry 563 (2004) 81–89.
[5] S. Sen Gupta, J. Datta, Journal of Electroanalytical Chemistry 594 (2006) 65–72.
[6] N. Fujiwara, K.A. Friedrich, U. Stimming, Journal of Electroanalytical Chemistry 472 (1999) 120–125.
[7] J. Souza-Garcia, E. Herrero, J.M. Feliu, ChemPhysChem 11 (2010) 1391–1394.
[8] E. Leiva, T. Iwasita, E. Herrero, J.M. Feliu, Langmuir 13 (1997) 6287.
[9] A. Sáez, E. Expósito, J. Solla-Gullón, V. Montiel, A. Aldaz, Electrochimica Acta 63 (2012) 105–111.
[10] E. Herrero, A. Fernández-Vega, J.M. Feliu, A. Aldaz, Journal of Electroanalytical Chemistry 350 (1993) 73–88.
[11] V. Del Colle, A. Berna, G. Tremiliosi-Filho, E. Herrero, J.M. Feliu, Physical Chemistry Chemical Physics 10 (2008) 3766.
[12] V. Del Colle, V. Santos, G. Tremiliosi-Filho, Electrocatalysis 1 (2010) 144–158.
[13] V. Del Colle, J. Souza-Garcia, G. Tremiliosi-Filho, E. Herrero, J.M. Feliu, Physical Chemistry Chemical Physics 13 (2011) 12163.
[14] A. López-Cudero, J. Solla-Gullón, E. Herrero, A. Aldaz, J.M. Feliu, Journal of Electroanalytical Chemistry 644 (2010) 117–126.
[15] J. Solla-Gullón, A. Rodes, V. Montiel, A. Aldaz, J. Clavilier, Journal of Electroanalytical Chemistry 554–555 (2003) 273–284.
[16] Q. Chen, J. Solla-Gullón, S. Sun, J.M. Feliu, Electrochimica Acta 55 (2010) 7982–7994.
[17] M. Figueiredo, F.J. Vidal-Iglesias, J. Solla-Gullón, V. Climent, J.M. Feliu, Zeitschrift für Physikalische Chemie 226 (2012) 901.
[18] F.J. Vidal-Iglesias, A. López-Cudero, J. Solla-Gullón, J.M. Feliu, Angewandte Chemie International Edition 52 (2013) 964–967.
[19] J. Lovic, A. Tripkovic, K. Popovic, Journal of the Serbian Chemical Society 76 (2011) 1523.
[20] Y. Huang, J. Cai, Y. Guo, Applied Catalysis B 129 (2013) 549–555.
[21] S. Motoo, M. Watanabe, Journal of Electroanalytical Chemistry 111 (1980) 261–268.
[22] R. Parsons, T. VanderNoot, Journal of Electroanalytical Chemistry 257 (1988) 9–45.
[23] T. Bligaard, J.K. Nørskov, Electrochimica Acta 52 (2007) 5512–5516.
[24] T. Iwasita, E. Pastor, Electrochimica Acta 39 (1994) 531–537.
[25] S. Chumillas, C. Busó-Rogero, J. Solla-Gullón, F.J. Vidal-Iglesias, E. Herrero, J.M. Feliu, Electrochemistry Communications 13 (2011) 1194–1197.
[26] F. Colmati, G. Tremiliosi-Filho, E.R. Gonzalez, A. Berna, E. Herrero, J.M. Feliu, Faraday Discussions 140 (2009) 379.
[27] L. Wen-Feng, L. Shi-Gang, T. Zhao-Wu, Journal of Electroanalytical Chemistry 364 (1994) 1–7.
[28] V. Climent, N. García-Araez, J.M. Feliu, in: M.T.M. Koper (Ed.), Fuel Cells Catalysis: A Surface Science Approach, John Wiley & Sons, Inc., New Jersey, 2009, p. 209.
[29] Q. Chen, F.J. Vidal-Iglesias, J. Solla-Gullon, S. Sun, J.M. Feliu, Chemical Science 3 (2012) 136.
[30] S. Chang, M.J. Weaver, Surface Science 241 (1991) 11–24.
[31] A. Santasalo-Aarnio, S. Tuomi, K. Jalkanen, K. Kontturi, T. Kallio, Electrochimica Acta 87 (2013) 730–738.
[32] S. Sun, S. Chen, N. Li, G. Lu, B. Chen, F. Xu, Colloids and Surfaces A: Physicochemical and Engineering Aspects 134 (1998) 207–220.
[33] V. Climent, E. Herrero, J.M. Feliu, Electrochimica Acta 44 (1998) 1403–1414.
[34] B. Peng, J. Wang, H. Zhang, Y. Lin, W. Cai, Electrochemistry Communications 11 (2009) 831–833.
[35] N. Kizhakevariam, M.J. Weaver, Surface Science 310 (1994) 183–197.
[36] S.C.S. Lai, M.T.M. Koper, Faraday Discussions 140 (2009) 399.
[37] X.H. Xia, H.-D. Liess, T. Iwasita, Journal of Electroanalytical Chemistry 437 (1997) 233–240.
[38] T. Iwasita, B. Rasch, E. Cattaneo, W. Vielstich, Electrochimica Acta 34 (1989) 1073–1079.
[39] J. Shin, W.J. Tornquist, C. Korzeniewski, C.S. Hoaglund, Surface Science 364 (1996) 122–130.
[40] D. Tarnowski, C. Korzeniewski, Journal of Physical Chemistry B 101 (1997) 253.